ISSN 2664-4169 (Print) & ISSN 2664-7923 (Online)
South Asian Research Journal of Biology and Applied Biosciences
Abbreviated Key Title: South Asian Res J Bio Appl Biosci

| Volume-8 | Issue-3 | May-June-2026 | **DOI: https://doi.org/10.36346/sarjbab.2026.v08i03.014**

Original Research Article

Ginseng-Mediated Green Synthesis of Selenium Nanoparticles: Antibacterial Activity against Ciprofloxacin-Resistant Clinical *Pseudomonas aeruginosa* and Effects on Povidone-Iodine and Ciprofloxacin

Sadiq Reda Mohammed[1]*, Amira Imran Hussien[2]

[1]Al-Qasim Green University, College of Biotechnology, Iraq

***Corresponding Author:** Sadiq Reda Mohammed
Al-Qasim Green University, College of Biotechnology, Iraq

Article History
Received: 11.03.2026
Accepted: 29.05.2026
Published: 16.06.2026

Abstract: Pseudomonas aeruginosa is an opportunistic pathogen with high levels of antibiotic resistance, which necessitates alternate antibacterial strategies. This study aimed to green-synthesize selenium nanoparticles (SeNPs) using aqueous Panax ginseng root extract and to test their antibacterial activities against ciprofloxacin-resistant clinical P. aeruginosa isolates, alone and in combination with povidone-iodine (PVP-I) and ciprofloxacin. The nanomaterials were characterised by Fourier-transform infrared spectroscopy (FTIR), UV–Visible spectroscopy, scanning electron microscopy (SEM), and X-ray diffraction (XRD). The synthesised SeNPs displayed an absorbance maximum at 303–305 nm, typical particle size of 36.02–46.80 nm and partly crystalline structure with the major XRD peak at 2θ = 28.323°. The SeNPs showed minimum inhibitory concentrations (MICs) of 25–50 µg/mL. The addition of these improved the antibacterial activity of PVP-I, lowering its MIC from 625–1250 to 300 µg/mL ($P < 0.001$), whereas the MIC of ciprofloxacin was unaffected ($P = 1.00$) at 12.5 µg/mL. These results provide evidence for the antibacterial activity of P. ginseng-mediated SeNPs against ciprofloxacin-resistant P. aeruginosa, especially in conjunction with PVP-I.

Keywords: Selenium Nanoparticles, *Panax Ginseng*, Green Synthesis, *Pseudomonas Aeruginosa*, Povidone–Iodine, Ciprofloxacin, Antibacterial Activity, MIC.

1. INTRODUCTION

Pseudomonas aeruginosa is a Gram-negative opportunistic bacterium and is one of the leading causes of hospital-acquired diseases. The therapeutic significance is associated with many resistance mechanisms, such as a reduction of outer-membrane permeability, multidrug efflux systems, beta-lactamase production, chromosomal modifications and biofilm formation [1–5]. Resistance to ciprofloxacin may emerge from target site mutations, overproduction of efflux pumps, reduced permeability and biofilm-associated mechanisms [6–8]. Povidone-iodine is widely used for infection control, however variations in sensitivity and adaptation to antiseptic exposure have been reported.[9)]

There is increasing interest in selenium nanoparticles (SeNPs) due to their antibacterial and antibiofilm activity, notably against *P. aeruginosa (*10*).* In addition, their antibacterial capabilities have been investigated along with other antimicrobial agents such as antibiotic-loaded or antibiotic-conjugated SeNPs against resistant bacteria [11, 12]. The plant-mediated green synthesis is a very simple and eco-friendly technique, where phytochemicals may act as reducing and stabilizing agents during the formation of SeNPs (13–15). Panax ginseng is rich in bioactive components such as ginsenosides and polysaccharides and hence offers a rich phytochemical profile for plant-mediated synthesis of nanoparticles*(*16*)*.

While the interest in plant-mediated SeNPs is on the rise, data on P. ginseng-mediated SeNPs and their antibacterial effectiveness against clinical *P. aeruginosa,* especially in conjunction with conventional antimicrobial treatments, remains sparse. Thus, the present work was aiming to synthesize SeNPs using an aqueous P. ginseng root

Copyright © 2026 The Author(s): This is an open-access article distributed under the terms of the Creative Commons Attribution **4.0 International License (CC BY-NC 4.0)** which permits unrestricted use, distribution, and reproduction in any medium for non-commercial use provided the original author and source are credited.

extract and characterize the synthesized nanoparticles using FTIR, UV–Visible spectroscopy, SEM and XRD. The antibacterial effect against clinical isolates of *P. aeruginosa* from ciprofloxacin-resistant patients was examined both alone and in combination with ciprofloxacin and povidone-iodine.

2. MATERIAL AND METHOD

2.1 Sample Collection, Identification, and Antimicrobial Susceptibility Testing of *Pseudomonas Aeruginosa*

Three hundred clinical specimens including burn and wound swabs, urine, sputum, blood and ear swabs were collected aseptically from patients with probable P. aeruginosa infections in hospitals of Babylon Governorate, Iraq. Specimens were transferred to the laboratory and processed 2–4 h after collection, cultivated on cetrimide, MacConkey and blood agar and incubated aerobically at 37°C for 24–48 h. Presumptive isolates of *P. aeruginosa* were identified using cultural, microscopic and biochemical features [17]. Antimicrobial susceptibility testing was conducted using VITEK® 2 Compact system (bioMérieux, France) using AST cards as per manufacturer's instructions [18]. Isolates were categorised according to CLSI breakpoints [19, 20]. Among 29 verified P. aeruginosa isolates, 20 were resistant and 9 were susceptible. Three ciprofloxacin resistant isolates with extensive resistance profiles were selected for further SeNP evaluation.

2.2 Preparation of the Aqueous Extract of Panax ginseng Roots

Aqueous root extract of Panax ginseng was produced using the Soxhlet extraction with modifications from earlier *P. ginseng* extraction techniques [21, 22]. Briefly, 5 g of finely powdered roots were extracted with 100 mL of distilled water at 100°C for 2 h, cooled, filtered through Whatman No. 1 filter paper, placed into sterile amber bottles and kept at 4°C until use.

2.2.1 Characterization of *P. ginseng* Extract

The functional groups involved in SeNP production were identified by FTIR analysis using a Shimadzu FTIR spectrophotometer with a resolution of 4 cm^{-1} in the range of 4000–400 cm^{-1} with 32 scans [23, 24]. The extract was characterized for optical absorption by recording the UV–Visible spectra in the range of 200–1100 nm using distilled water as the blank.[25]

2.3 Preparation of Selenium Nanoparticles (SeNPs)

SeNPs were synthesized by employing the aqueous extract of Panax ginseng root as a reducing and stabilizing agent based on the modified plant-mediated method [13, 14]. Briefly, 50 mL of 0.0265 M sodium selenite (Na_2SeO_3) was heated at 90°C for 15 min and then added dropwise with newly made P. ginseng extract (50 mL). The mixture was kept at 90 °C for 2 h, brick red to deep red colour formed after ~30 min suggesting the creation of SeNPs. The suspension was cooled, transferred to sterile amber containers and kept at 4°C until characterisation and anti-microbial test.

Characterization of Selenium Nanoparticles (SeNPs) 42

2.4.1 FTIR Analysis

The functional groups involved in the synthesis and stabilization of SeNPs were identified using FTIR spectroscopy. The spectra of the synthesized SeNPs and P. ginseng extract were recorded in the 4000–400 cm^{-1} range and examined for variations in typical absorption bands [15- 24]

2.4.2 UV–Visible Spectroscopy Analysis

UV–Visible spectroscopy was used for assessment of optical properties and first indication of SeNP production. The absorption spectra of the nanoparticle solution were recorded and analyzed according to the location and form of the distinctive absorption band [10-14].

2.4.3 Scanning Electron Microscopy (SEM)

The shape, particle size and aggregation of the synthesized SeNPs were evaluated by SEM. Surface characteristics and diameter of the nanoscale particles were determined by analyzing high resolution micrographs [26-28].

2.4.4 X-ray Diffraction (XRD)

The XRD examination was conducted to analyze crystalline structure and phase nature of synthesized SeNPs . The crystalline structure of the synthesized nanoparticles was assessed by looking at the diffraction peaks at certain values of 2θ and compared with the published selenium diffraction patterns [27-29].

2.5 Antimicrobial Activity

2.5.1 Determination of the Minimum Inhibitory Concentration (MIC)

Minimum inhibitory concentration of selenium nanoparticles, ciprofloxacin and povidone-iodine against three clinical strains of P. Pseudomonas aeruginosa isolates were tested by broth microdilution in sterile 96-well plates using CLSI standards with minor modifications for testing nanoparticles [12-30]. Functional solutions of SeNPs, CIP and PVP-I were prepared at 100, 25 and 5000 µg/mL, respectively, and serially diluted in Mueller–Hinton broth. A bacterial

inoculum of a similar quantity (~ 1 × 10^6 CFU/mL) was added to obtain a final volume of 200 µL, giving an approximate bacterial concentration of 5 × 10^5 CFU/mL in each well. The final concentrations were ranging from 50.0 to 0.8 µg/mL for SeNPs, from 12.50 to 0.39 µg/mL for CIP and from 2500 to 78.13 µg/mL for PVP-I. Positive and negative controls were also present. The plates were incubated at 37°C for 18-24 hours, and the minimum inhibitory concentration (MIC) was defined as the lowest compound concentration with no visible growth. All trials were performed in triplicates.

2.5.2 Effect of SeNPs on the MIC of Povidone–Iodine and Ciprofloxacin

The impact of SeNPs on MICs of PVP-I and CIP against three clinical P. aeruginosa isolates was studied using a broth microdilution-based combination test [12-31]. Triplicate testing was performed on each isolate. Briefly, 50 µL of antimicrobial solution was mixed with 100 µL of bacterial inoculum standardized to 0.5 McFarland containing SeNPs to provide a final volume of 150 µL/well and a final concentration of SeNPs of 10 µg/mL. The concentrations of PVP-I were 1250, 875, 612.5, 428.7, 300.1 and 210 µg/mL while the concentrations of CIP were 12.5, 9.4, 7.0, 5.3, 4.0 and 3.0 µg/mL. Parallel wells without SeNPs as well as proper growth and sterility controls were provided. Plates were incubated at 37°C for 18–24 h and the MIC was recorded as the lowest dose fully preventing observable growth.

2.6 Statistical Analysis

The data were analyzed using IBM SPSS Statistics and Microsoft Excel**.** Results were given as mean ± standard deviation (SD) wherever appropriate. Statistical significance was considered at $P < 0.05$. Microsoft Excel was used to organize and graphically portray data.

3. RESULTS

3.1. FTIR Analysis

The notable bands were altered from 3377.36, 2926.01, 1629.85, 1413.82, and 1240.23 cm^{-1} in the extract to 3412.08, 2922.16, 1598.99, 1409.96, and 1205.51 cm^{-1} in the SeNPs, respectively, indicating the obvious spectrum changes after synthesis.

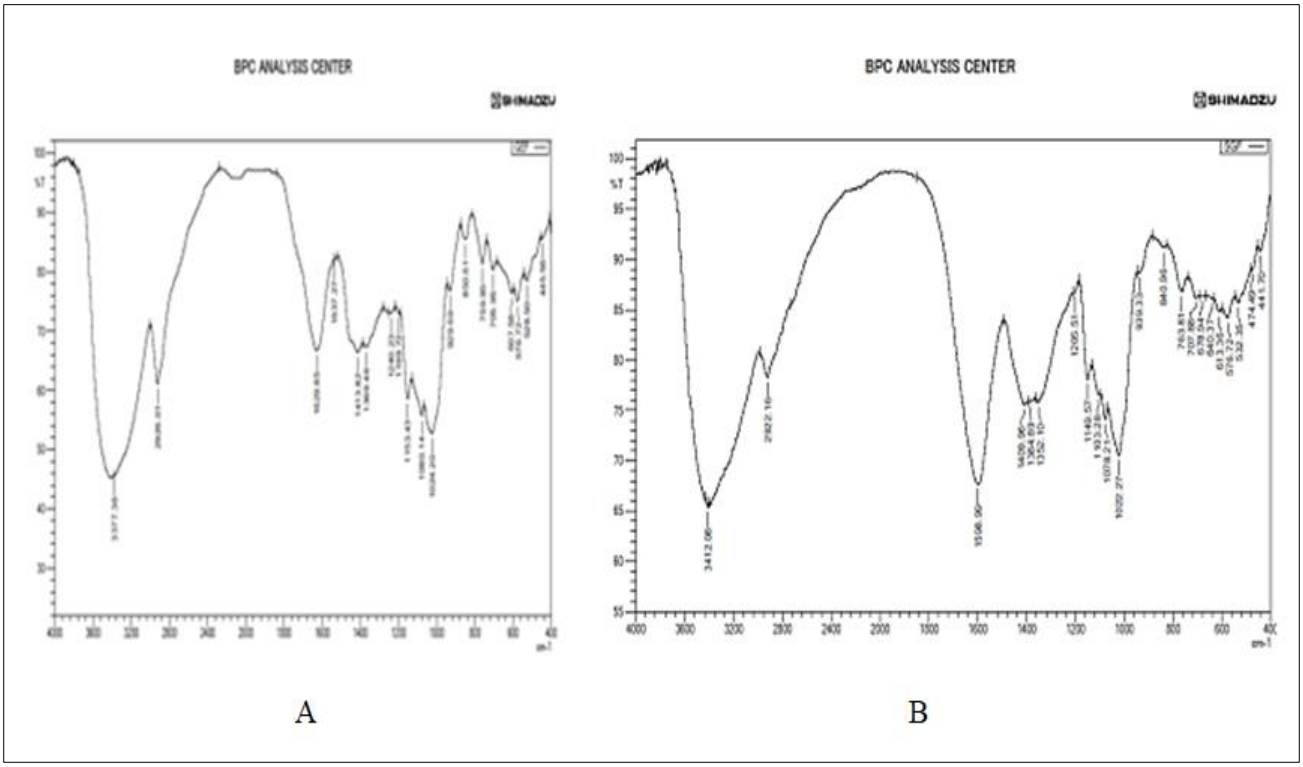

Figure 1: FTIR spectra of (A) *Panax ginseng* root extract and (B) green-synthesized SeNPs.

3.2. UV–Visible Spectroscopy

The optimum absorption range of P. ginseng extract was observed at 315-320 nm while the synthesized SeNPs showed absorption peak at 303-305 nm. The SeNP spectra likewise showed a more intense absorption band with a little shoulder about 580–590 nm.

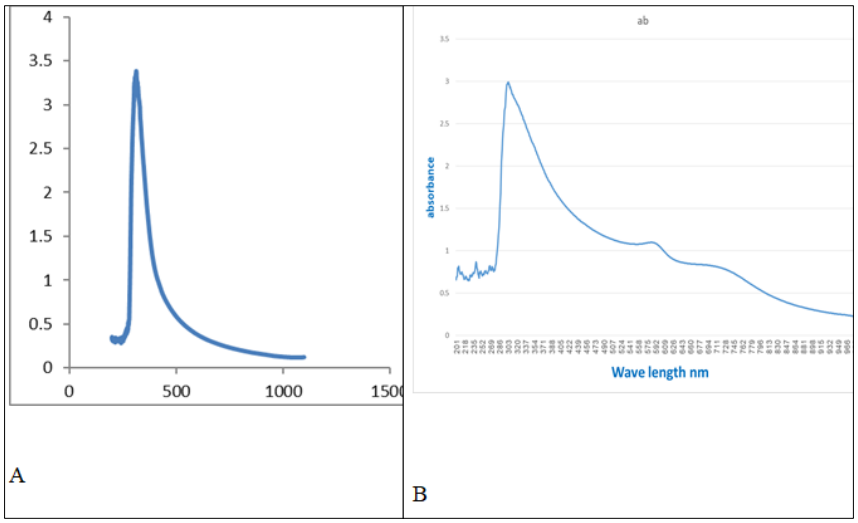

Figure 2: UV–Visible absorption spectra of (A) *Panax ginseng* root extract and (B) green-synthesized SeNPs.

3.3. SEM Analysis

SEM images showed heterogeneous aggregated formations with smaller particles at increased magnification. The mean particle sizes were in the range 36.02–46.80 nm with significant agglomeration.

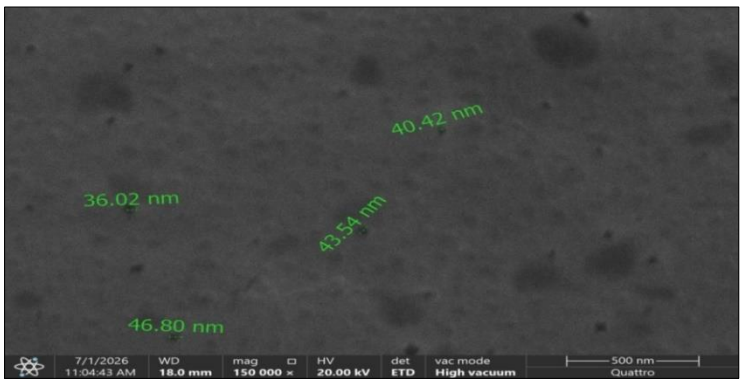

Figure 3: SEM micrographs of green-synthesized SeNPs at different magnifications, showing particle morphology and aggregation

3.4. XRD Analysis

The XRD pattern showed a strong diffraction peak at 2θ=28.323° with weaker reflections at larger angles and a wide background, which indicates the presence of a crystalline component with a high degree of structural disorder.

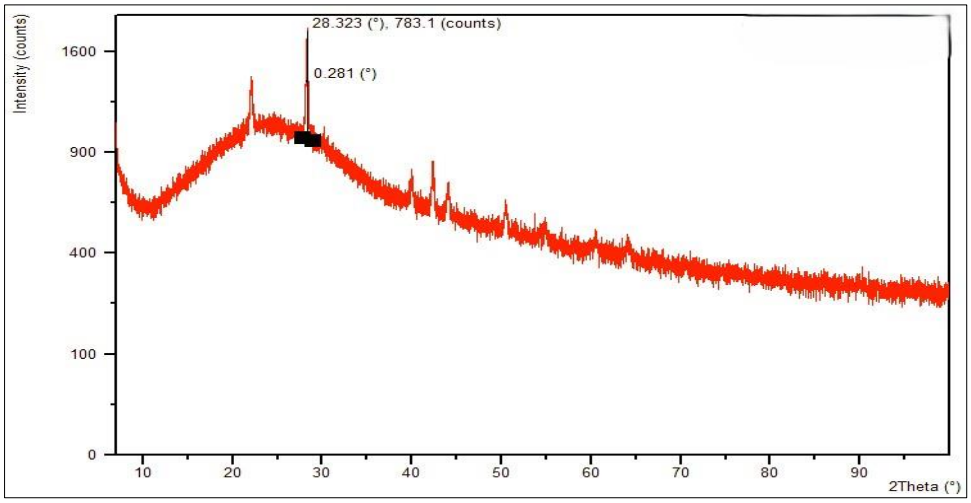

Figure 4: XRD pattern of green-synthesized SeNPs.

3.5. Minimum Inhibitory Concentration (MIC)

Table 1: MICs of SeNPs, PVP-I, and CIP against the three clinical isolates of P. aeruginosa. The MICs of SeNP were 50 µg/mL for isolate 1 and 25 µg/mL for isolates 2 and 3. The MICs of PVP-I were 625, 1250 and 1250 µg/ml correspondingly while for CIP the MIC was 12.5 µg/ml for all isolates. Representative broth microdilution plates are presented in Fig. 1.

Table 1: MICs of SeNPs, PVP-I, and ciprofloxacin against three clinical *Pseudomonas aeruginosa* isolates

Isolate	POV mic (ug/ml)	cip mic (ug/ml)	Se mic (ug/ml)
1	625	12.5	50
2	1250	12.5	25
3	1250	12.5	25

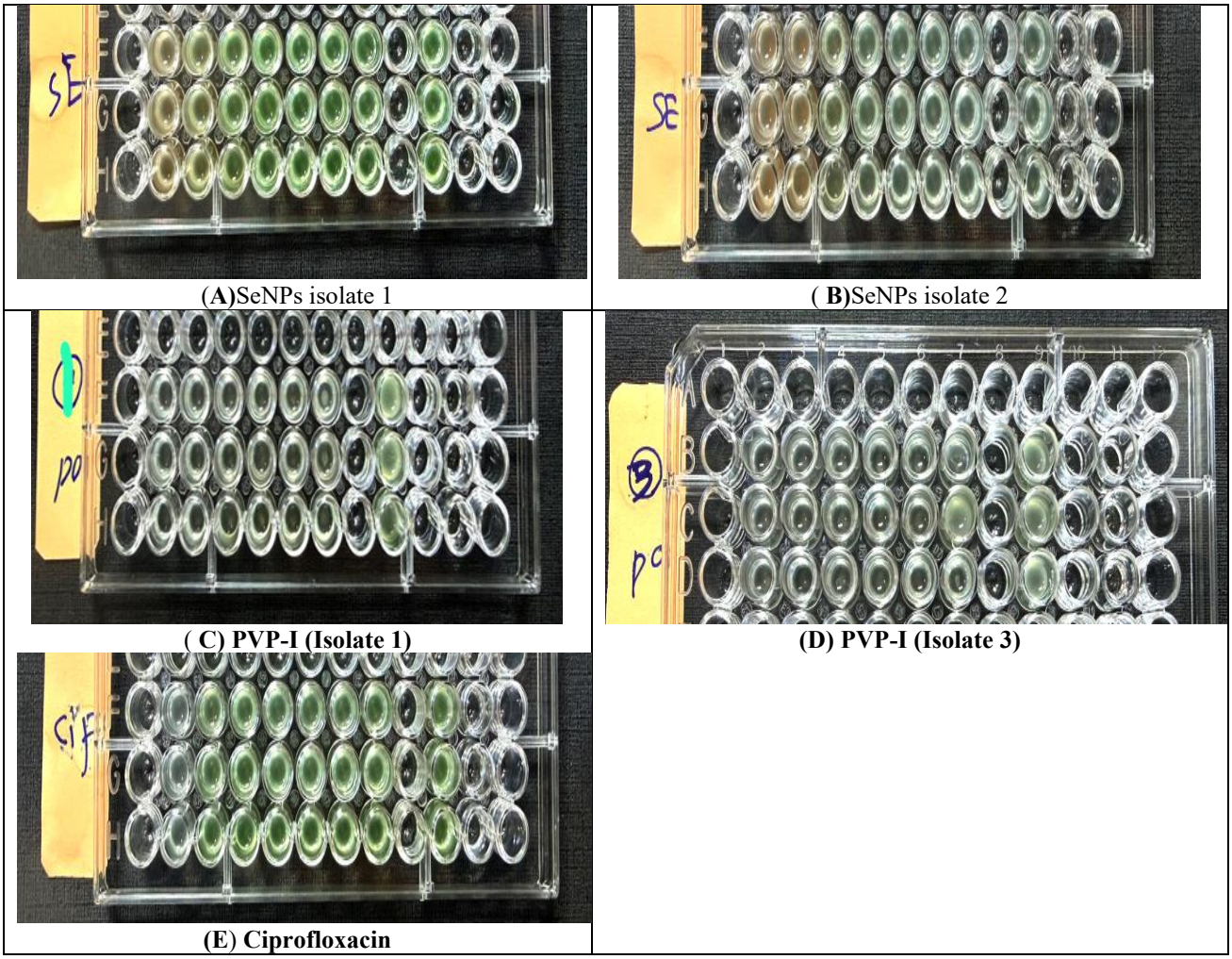

(A) SeNPs isolate 1

(B) SeNPs isolate 2

(C) PVP-I (Isolate 1)

(D) PVP-I (Isolate 3)

(E) Ciprofloxacin

Figure 5: Representative broth microdilution plates for MIC determination of SeNPs, PVP-I, and ciprofloxacin against P. aeruginosa

3.6. Effect of SeNPs on PVP-I and Ciprofloxacin Activity

The presence of SeNPs enhanced the activity of PVP-I, decreasing its MIC from 625 to 300 µg/mL in isolate 1 and from 1250 to 300 µg/mL in isolates 2 and 3 ($P < 0.001$). However, no change was seen in CIP activity of SeNPs at MIC of 12.5 µg/mL in all isolates ($P = 1.00$) (Tables 2 and 3; Figures 2 and 3).

Table 2: Effect of SeNPs on the MIC of PVP-I against P. aeruginosa clinical isolates

Mic(ug/ml)	pov	pov+se	Chi square	P value
1	625	300	70.1	0.001
2	1250	300		
3	1250	300		

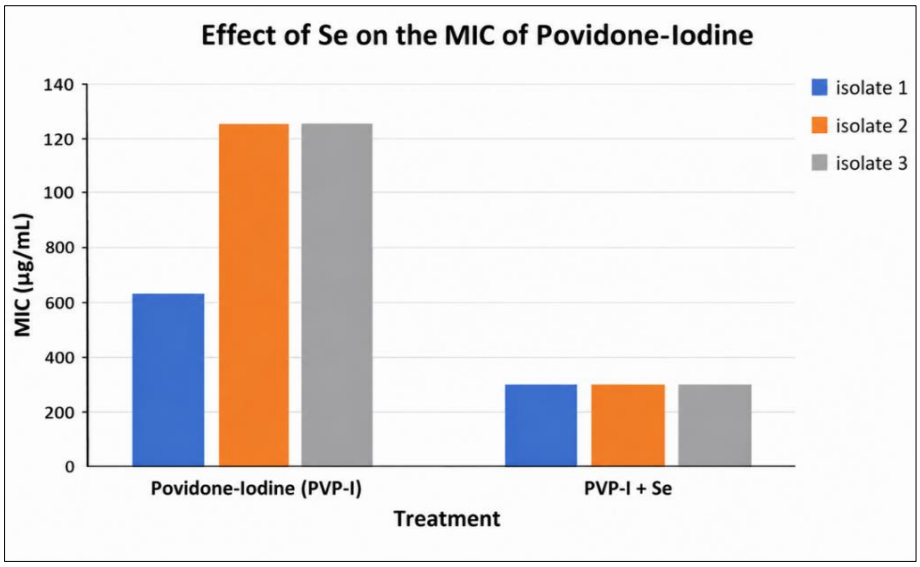

Figure 6: Effect of SeNPs on the MIC of PVP-I against *P. aeruginosa* clinical isolates

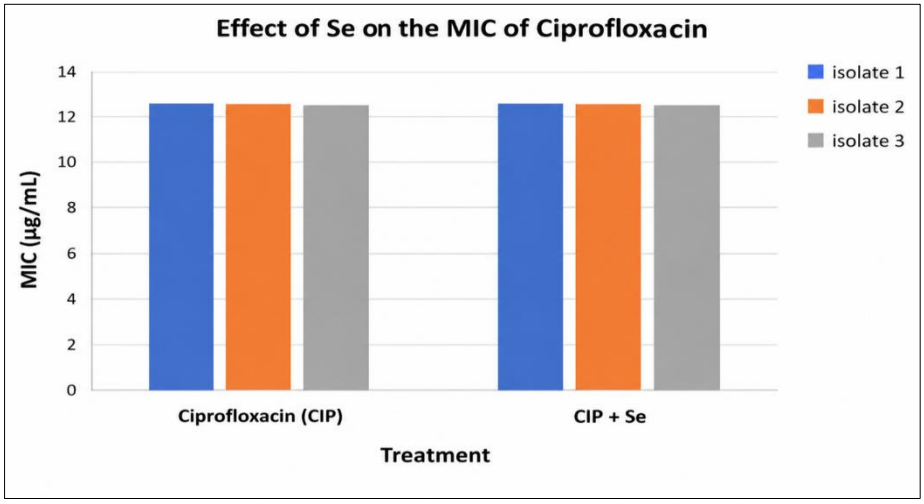

Figure 7: Effect of SeNPs on the MIC of Ciprofloxacin against *P. aeruginosa* clinical isolates

Table 3: Effect of SeNPs on the MIC of Ciprofloxacin against Psedomonas aeruginosa Clinical Isolates

Mic (ug/ml)	Cip	cip+se	Chi square	P value
isolate 1	12.5	12.5	0.00	1.00
isolate 2	12.5	12.5		
isolate 3	12.5	12.5		

4. DISCUSSION

The physicochemical properties of the green synthesised selenium nanoparticles (SeNPs) by Panax ginseng root extract were determined by FTIR, UV-Visible spectroscopy, SEM, and XRD. The results showed spectrum alterations after synthesis, creation of aggregated nanoscale structures, unique UV-Visible absorption profile and a partly crystalline structure. Collectively, the phytochemicals found in P. ginseng include ginsenosides, polysaccharides and polyphenols might be responsible for reduction of selenite ions and stabilisation of the resultant nanoparticles. But the physicochemical features of plant-mediated SeNPs may also be modified by the plant composition and synthesis conditions [14-32].

FTIR analysis showed considerable changes in the absorption bands of P. ginseng extract following the synthesis of SeNP. The bands at 3377.36, 2926.01, 1629.85, 1413.82, and 1240.23 cm^{-1} were shifted to 3412.08, 2922.16, 1598.99, 1409.96, and 1205.51 cm^{-1}, respectively. These alterations suggest the possible role of hydroxyl and other oxygen- and nitrogen-containing functional groups in the reduction of selenium and stability of the SeNP surfaces [14-33].

The UV–Visible spectral analysis of P. ginseng extract revealed absorption at 315–320 nm and the synthesized SeNPs showed shifted absorption maxima at 303–305 nm with larger absorption and faint shoulder at 580–590 nm. These

variations imply changed optical characteristics after nanoparticle formation, and may be a consequence of modifications in particle size, morphology, surface chemistry, and aggregation [14]. The measured absorption maximum was equivalent to the 305 nm peak reported for SeNPs mediated by Ananas comosus peel and near to the 310 nm peak reported for Blighia sapida-mediated SeNPs [34, 35]. The weak shoulder at 580–590 nm might be attributed to aggregation of particles or heterogeneity of the particle size and surface characteristics. These variations in plant-mediated SeNPs can be due to the variances in phytochemical content and synthesis circumstances [14-35].

SEM analysis revealed the formation of aggregated nanoscale structures with diameters ranging from 36.02 nm to 46.80 nm. This range of the size was comparable with the 28–50 nm spherical SeNPs with high agglomeration seen in a previous plant-mediated synthesis [36], and almost identical with the 38 nm SeNPs synthesized by sodium selenite, Prunus persica leaf extract and Aloe vera gel as a stabilizer [37]. In contrast, the uncoated SeNPs reported for Panax ginseng were in the size range of 50–150 nm, but the glycol-chitosan coating caused the production of larger aggregates [38]. These differences might be due to variations in plant phytochemicals, the ratio of precursor to extract, reaction conditions, stabilizing agents and surface chemistry, all of which may affect the formation and aggregation of nanoparticles [14].

The XRD pattern showed a major diffraction peak at $2\theta = 28.323°$ and minor reflections at higher angles, in addition to a normal wide background. This pattern shows the presence of a partly crystalline substance with some structural irregularity. The prominent diffraction peak was near the reported reflection at ~29.70° for plant-mediated SeNPs synthesized using Nyctanthes arbor-tristis extract [39]. Differences in the peak locations, intensities and the overall diffraction patterns may be attributed to differences in particle size, crystallite structure, plant derived capping compounds and synthesis circumstances which may affect selenium nucleation and crystal growth [14-39].

The synthesized SeNPs showed antibacterial efficacy against all tested ciprofloxacin resistant Pseudomonas aeruginosa isolates with MIC values between 25 and 50 µg/mL. The greatest MIC was observed for isolate 1 (50 µg/mL) whereas isolates 2 and 3 had lower MIC values (25 µg/mL) demonstrating variance in susceptibility across the tested isolates. These results are in general agreement with earlier studies of antibacterial activity of plant mediated SeNPs against P. aeruginosa. However, MIC values should be directly compared with caution, as the antibacterial activity might be dependent on nanoparticle size, shape, surface chemistry, synthesis circumstances, test technique, and bacterial strain [10-33].

The addition of SeNPs improved the activity of PVP-I against the three P. aeruginosa isolates, decreasing the MIC from 625 to 300 µg/mL in isolate 1 and from 1250 to 300 µg/mL in isolates 2 and 3. The result may correlate to interactions between SeNPs and the bacterial surfaces, which may enhance the sensitivity of bacteria to PVP-I. Similarly, a prior research revealed that SeNP–PVP-I combinations increased bactericidal activity and decreased MIC and MBC values against S. aureus and methicillin-resistant S. aureus (MRSA), however that study was performed on Gram-positive bacteria rather than P. aeruginosa [40]. The primary mechanism of action of PVP-I is the liberation of free iodine, which may penetrate microbial cells and oxidise essential biological molecules [41]. Furthermore, certain SeNP-based formulations shown enhanced antibacterial activity against resistant microorganisms [12-31]. However, the MIC of ciprofloxacin was uniform (12.5 µg/mL) for all the isolates and was unaffected by SeNPs. This variable response shows that the effect of SeNP incorporation depended on the agent and may have been influenced by the antibacterial mechanism, properties of the nanoparticles, bacterial strain and conditions of the experiment.

5. CONCLUSION

Synthesis and characterization of SeNPs assisted by Panax ginseng were carried out using FTIR, UV-visible spectroscopy, SEM and XRD. The SeNPs demonstrated antibacterial efficacy against ciprofloxacin-resistant P. aeruginosa MICs of 25–50 µg/mL and increased PVP-I activity. However, no such increase was seen with ciprofloxacin. These data confirm the potential of P. ginseng-mediated SeNPs as an antibacterial approach, particularly in combination with PVP-I.

REFERENCES

1. Pachori P, Gothalwal R, Gandhi P. Emergence of antibiotic resistance Pseudomonas aeruginosa in intensive care unit; a critical review. Genes Dis. 2019;6(2):109–19.
2. Diggle SP, Whiteley M. Microbe Profile: Pseudomonas aeruginosa: opportunistic pathogen and lab rat. Microbiology. 2020;166(1):30–3.
3. Reynolds D, Kollef M. The epidemiology and pathogenesis and treatment of Pseudomonas aeruginosa infections: an update. Drugs. 2021;81(18):2117–31.
4. Qin S, Xiao W, Zhou C, Pu Q, Deng X, Lan L, et al. Pseudomonas aeruginosa: pathogenesis, virulence factors, antibiotic resistance, interaction with host, technology advances and emerging therapeutics. Signal Transduct Target Ther. 2022;7(1):199.
5. Abed HS, Hosseini SM, Jassim ZM. Immunological and molecular detection of biofilm formation and antibiotic resistance genes of Pseudomonas aeruginosa isolated from urinary tract. Iran J Microbiol. 2025;17(3):376.

6. Pang Z, Raudonis R, Glick BR, Lin T-J, Cheng Z. Antibiotic resistance in Pseudomonas aeruginosa: mechanisms and alternative therapeutic strategies. Biotechnol Adv. 2019;37(1):177–92.
7. Laborda P, Hernando-Amado S, Martínez JL, Sanz-García F. Antibiotic resistance in Pseudomonas. In: Pseudomonas aeruginosa: Biology, Pathogenesis and Control Strategies. Springer; 2022. p. 117–43.
8. Yamasaki S, Zwama M, Yoneda T, Hayashi-Nishino M, Nishino K. Drug resistance and physiological roles of RND multidrug efflux pumps in Salmonella enterica, Escherichia coli and Pseudomonas aeruginosa. Microbiology. 2023;169(6):1322.
9. Karpiński TM, Korbecka-Paczkowska M, Stasiewicz M, Mrozikiewicz AE, Włodkowic D, Cielecka-Piontek J. Activity of antiseptics against Pseudomonas aeruginosa and its adaptation potential. Antibiotics. 2025;14(1):30.
10. Thamayandhi C, El-Tayeb MA, Syed SRM, Sivaramakrishnan R, Gunasekar B. Antibacterial and anti-biofilm efficacy of selenium nanoparticles against Pseudomonas aeruginosa: Characterization and in vitro analysis. Microb Pathog. 2024;196:106998.
11. Hasan MF, Al-Awady MJ. The impact of berberine loaded selenium nanoparticles on K. pneumoniae and Candida albicans antibiotics resistance isolates. Arch Razi Inst. 2023;78(3):1005.
12. Ridha DM, Al-Awady MJ, Abd Al-Zwaid AJ, Balakit AA, Al-Dahmoshi HOM, Alotaibi MH, et al. Antibacterial and antibiofilm activities of selenium nanoparticles-antibiotic conjugates against anti-multidrug-resistant bacteria. Int J Pharm. 2024;658:124214.
13. Sentkowska A, Konarska J, Szmytke J, Grudniak A. Herbal polyphenols as selenium reducers in the green synthesis of selenium nanoparticles: Antibacterial and antioxidant capabilities of the obtained SeNPs. Molecules. 2024;29(8):1686.
14. Pyrzynska K. Plant extracts for production of functionalized selenium nanoparticles. Materials (Basel). 2024;17(15):3748.
15. Pyrzynska K, Sentkowska A. Biosynthesis of selenium nanoparticles using plant extracts. J Nanostructure Chem. 2022;12(4):467–80.
16. Ding M, Cheng H, Li X, Li X, Zhang M, Cui D, et al. Phytochemistry, quality control and biosynthesis in ginseng research from 2021 to 2023: A state-of-the-art review concerning advances and challenges. Chinese Herb Med. 2024;16(4):505–20.
17. Tille PM. Bailey & Scott's Diagnostic Microbiology-E-Book: Bailey & Scott's Diagnostic Microbiology-E-Book. Elsevier Health Sciences; 2013.
18. Moehario LH, Tjoa E, Putranata H, Joon S, Edbert D, Robertus T. Performance of TDR-300B and VITEK® 2 for the identification of Pseudomonas aeruginosa in comparison with VITEK®-MS. J Int Med Res. 2021;49(2):0300060521989893.
19. Nstitute C and LS. No TitleMethods for Dilution Antimicrobial Susceptibility Tests for Bacteria That Grow Aerobically. Wayne, PA; 2024.
20. Roy C, Vandana WV, Machado S, CY R. A Retrospective Analysis of Bacteriological Profile and Antimicrobial Susceptibility Trends of Pus Isolates from Outpatients Departments in a Tertiary Care Hospital. Int J Med Pharm Res. 2026;7:1702–8.
21. Yue Y, Qiu Z-D, Qu X-Y, Deng A-P, Yuan Y, Huang L-Q, et al. Discoursing on Soxhlet extraction of ginseng using association analysis and scanning electron microscopy. J Pharm Anal. 2018;8(5):312–7.
22. Jegal J, Jeong EJ, Yang MH. A review of the different methods applied in ginsenoside extraction from Panax ginseng and Panax quinquefolius roots. Nat Prod Commun. 2019;14(9):1934578X19868393.
23. Yang Y, Ju Z, Yang Y, Zhang Y, Yang L, Wang Z. Phytochemical analysis of Panax species: a review. J Ginseng Res. 2021;45(1):1–21.
24. Al-Amin K, Kawsar M, Mamun MTRB, Sahadat Hossain M. Fourier transform infrared spectroscopic technique for analysis of inorganic materials: a review. Nanoscale Adv. 2025;7(21):6677–702.
25. Arif M, Raza H, Akhter T. UV-Vis spectroscopy in the characterization and applications of smart microgels and metal nanoparticle-decorated smart microgels: a critical review. RSC Adv. 2024;14(51):38120–34.
26. Zhang X, Zhao X, Li H, Hao X, Xu J, Tian J, et al. Detection methods of nanoparticles synthesized by Gas-Phase method: A review. Front Chem. 2022;10:845363.
27. Ibrahim SSS, Ansari YN, Puri A V, Patil V V, Gaikwad SS, Haroon RA. Recent progress in the green synthesis, characterization, and applications of selenium nanoparticles. Bio Integr. 2024;5(1):969.
28. Yilmaz MT, Ispirli H, Taylan O, Dertli E. A green nano-biosynthesis of selenium nanoparticles with Tarragon extract: Structural, thermal, and antimicrobial characterization. Lwt. 2021;141:110969.
29. Tabibi M, Aghaei S, Amoozegar MA, Nazari R, Zolfaghari MR. Characterization of green synthesized selenium nanoparticles (SeNPs) in two different indigenous halophilic bacteria. BMC Chem. 2023;17(1):115.
30. Wiegand I, Hilpert K, Hancock REW. Agar and broth dilution methods to determine the minimal inhibitory concentration (MIC) of antimicrobial substances. Nat Protoc. 2008;3(2):163–75.
31. Zeraatkar S, Tahan M, Sadeghian H, Nazari R, Behmadi M, Hosseini Bafghi M. Effect of biosynthesized selenium nanoparticles using nepeta extract against multidrug-resistant Pseudomonas aeruginosa and Acinetobacter baumannii. J Basic Microbiol. 2023;63(2):210–22.

32. Hussain A, Lakhan MN, Hanan A, Soomro IA, Ahmed M, Bibi F, et al. Recent progress on green synthesis of selenium nanoparticles–a review. Mater Today Sustain. 2023;23:100420.
33. Haseeb HA, Khan MA, Rasheed H, Zahid MU, Doan TD, Siddique MAR, et al. Polygonum bistorta Linn. as a green source for synthesis of biocompatible selenium nanoparticles with potent antimicrobial and antioxidant properties. BioMetals. 2024;37(6):1511–27.
34. Ibraheem O, Oyeniran OH, Ogundipe OM, Abe EO, Oyedepo TA, Sodeinde KO, et al. Photo-physical characterizations and evaluation of in-vitro antioxidant, anti-inflammatory and antidiabetic potentials of green synthesized ackee (Blighia sapida) selenium nano-particles. BMC Complement Med Ther. 2024;24(1):392.
35. Soliman MKY, Salem SS. Uncovering the potential of biofabricated Ananas comosus peel selenium nanoparticles for antibacterial, antibiofilm, suppression of virulence genes (can and LuxS), anticancer, and antioxidant properties. BMC Biotechnol. 2025;25(1):51.
36. Daler S, Korkmaz N, Kılıç T, Hatterman-Valenti H, Karadağ A, Kaya O. Modulatory effects of selenium nanoparticles against drought stress in some grapevine rootstock/scion combinations. Chem Biol Technol Agric. 2024;11(1):108.
37. Shayan S, Hajihajikolai D, Ghazale F, Gharahdaghigharahtappeh F, Faghih A, Ahmadi O, et al. Optimization of green synthesis formulation of selenium nanoparticles (SeNPs) using peach tree leaf extract and investigating its properties and stability. Iran J Biotechnol. 2024;22(3):e3786.
38. Abid S, Kaliraj L, Rahimi S, Kim YJ, Yang DC, Kang SC, et al. Synthesis and characterization of glycol chitosan coated selenium nanoparticles acts synergistically to alleviate oxidative stress and increase ginsenoside content in Panax ginseng. Carbohydr Polym. 2021;267:118195.
39. Satpathy S, Panigrahi LL, Samal P, Sahoo KK, Arakha M. Biogenic synthesis of selenium nanoparticles from Nyctanthes arbor-tristis L. and evaluation of their antimicrobial, antioxidant and photocatalytic efficacy. Heliyon. 2024;10(12).
40. Xiaojuan HE, Xueshi LUO, Jinying C, Guangchao YU, Jingxiang Z, Lihuan HOU. Bactericidal Effect of Selenium Nanoparticles Combined with Povidone-iodine on Pathogenic Bacteria in Surgical Site Infection. J Sun Yat-sen Univ (Medical Sci. 2024;45(2):206–15.
41. Lepelletier D, Maillard JY, Pozzetto B, Simon A. Povidone iodine: properties, mechanisms of action, and role in infection control and Staphylococcus aureus decolonization. Antimicrob Agents Chemother. 2020;64(9):10–1128.